Plant Stress 21 (2026) 101355

Contents lists available at ScienceDirect

Plant Stress

journal homepage: www.sciencedirect.com/journal/plant-stress

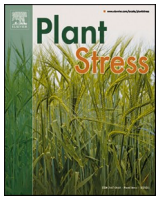

Drought effects on the leaf uptake of carbonyl sulfide and CO_2 in *Pinus sylvestris* and *Juniperus communis*

Anna de Vries [a,*], Felix M. Spielmann [a], Albin Hammerle [a], Judith Schmack [b], Werner Jud [b], Thomas Karl [b], Jörg-Peter Schnitzler [c], Jana Barbro Winkler [c], Georg Wohlfahrt [a]

[a] Department of Ecology, University of Innsbruck, 6020 Innsbruck, Austria
[b] Department of Atmospheric and Cryospheric Sciences, University of Innsbruck, 6020, Innsbruck, Austria
[c] Research Unit Environmental Simulation, Helmholtz Zentrum München, D-85764 Neuherberg, Germany

ARTICLE INFO

Keywords:
Gross primary productivity
Stomatal conductance
Controlled drought experiment
COS/OCS
Scots Pine
Common Juniper

ABSTRACT

Gross primary productivity (GPP) drives the land carbon sink, but its response to climate change and extreme weather events like drought remains uncertain. However, GPP cannot be measured directly but must be inferred through proxies, which introduces uncertainties that limit predictions. One promising approach is to measure carbonyl sulfide (COS) fluxes, supported by a thorough understanding of the relative uptake ratio between COS and CO_2, the leaf relative uptake (LRU). We derived plant-scale COS and CO_2 fluxes and calculated the LRU of *Pinus sylvestris* (pine) and *Juniperus communis* (juniper), under controlled drought conditions. The LRU remained constant (median daytime value of 1.47) in pine across the whole drought gradient due to opposing physiological processes: adjustment of conductances to COS and changes in the ratio of intercellular-to-ambient CO_2 concentration. In juniper, the LRU also had a constant value (daytime median of 1.41) for soil water content (SWC) above 17 % and increased with decreasing SWC below this threshold, driven by a decline in the stomatal to internal conductance to COS. Under drought stress, both COS and CO_2 uptake declined more in pine than in juniper. This study highlights LRU variability among species and water availability levels, providing insights into the underlying ecophysiological processes.

1. Introduction

Gross primary productivity (GPP) is the proximal driver for the net land carbon sink which currently removes around 1/4 of the annual anthropogenic carbon dioxide (CO_2) emissions (Friedlingstein et al., 2025). However, climate change, along with the increasing frequency of extreme events such as drought (Dai, 2013; Trenberth et al., 2014), may significantly alter GPP (IPCC, 2023). This is particularly important in mountainous regions, which are warming up twice as fast compared to the global average (IPCC, 2023; Orr et al., 2024; Pepin et al., 2025, 2022). Therefore, understanding how GPP responds to droughts in mountain regions is crucial for assessing regional carbon budgets. The literature indicates a substantial uncertainty in current estimates of the terrestrial carbon sink, particularly in areas of complex topography (Reif et al., 2024; Rotach et al., 2014). While observational data and vegetation models show significant global greening due to the CO_2 fertilization effect in the past (Piao et al., 2020), future responses of the land carbon sink to increasing temperature and CO_2 concentrations remain uncertain. Some studies suggest a significant weakening of the current sink. For example, Ke et al. (2025) reported a drastic decline during the 2023 El Nino year, and Friedlingstein et al. (2024) observed a decline over the last few decades.

Despite its importance, GPP cannot be measured directly at the ecosystem scale and must be indirectly estimated through diverse methods and models, an unavoidable limitation that adds substantial uncertainty to ecosystem carbon assessments (Wohlfahrt and Gu, 2015). This restricts our ability to project the impact of climate change on GPP, especially in relation to extreme events such as drought (Spielmann et al., 2019; Wohlfahrt and Gu, 2015).

A promising proxy for GPP are carbonyl sulfide (COS) fluxes (Eq. (1), Campbell et al. (2008). Plants take up COS in parallel to CO_2, but in contrast to the latter, it is generally not emitted and thus correlating with GPP (Asaf et al., 2013; Berry et al., 2013; Sandoval-Soto et al., 2005; Stimler et al., 2010; Whelan et al., 2018).

* Corresponding author.
E-mail address: anna.de-vries@uibk.ac.at (A. de Vries).

https://doi.org/10.1016/j.stress.2026.101355
Received 7 January 2026; Received in revised form 16 March 2026; Accepted 23 March 2026
Available online 23 March 2026

$$GPP = -F_{COS}\frac{\chi CO_2}{\chi COS}\frac{1}{LRU} \quad \text{(Eq. 1)}$$

with F_{COS} the measured COS flux (in units of pmol $m^{-2}s^{-1}$), χCO_2 and χCOS the atmospheric dry mole fractions of CO_2 and COS (in units of ppm and ppt), respectively, and LRU the dimensionless leaf relative uptake.

For this approach, the LRU, i.e., the ratio of the deposition velocities of COS over CO_2 (Sandoval-Soto et al., 2005), is crucial and must be defined beforehand. While early studies (Asaf et al., 2013; Berkelhammer et al., 2014; Stimler et al., 2010) determined an LRU value of approx. 1.6 for C_3 species, many other studies, particularly more recent ones, report a wider range of LRU values. Wohlfahrt et al. (2012) concluded that the LRU theoretically can range from 0.6 to 4.3. The synthesis study of Whelan et al. (2018) reports experimentally derived LRU values ranging from 0.7 to 6.2 (95 % confidence interval) with a median of 1.68. Spielmann et al. (2023) deduced that LRU values vary between soybean types and in response to drought stress conditions. These studies and a number of others (Kooijmans et al., 2019; Sun et al., 2022; Yang et al., 2018) suggest that the LRU varies among species and meteorological conditions like radiation, air humidity and soil moisture levels, and can introduce large errors if not addressed correctly in GPP estimations (Eq. (1)) (Wohlfahrt et al., 2023).

To better understand the drivers for differences in LRU, Eq. (1) can be re-arranged to Eq. (2) where the flux terms are replaced with the Fick's diffusion equations under the assumption that the boundary layer conductance is infinite (Seibt et al., 2010; Wohlfahrt et al., 2023).

$$\text{LRU} = \frac{1}{1.21}\left(\frac{1}{1+\frac{g_s^s}{g_i^s}}\right)\left(\frac{1}{1-\frac{C_i^c}{C_a^c}}\right) \quad \text{(Eq. 2)}$$

with 1.21^{-1} the conversion factor of stomatal conductance of COS to CO_2, g_s^s and g_i^s the stomatal and internal conductances to COS (in units of mmol $m^{-2}s^{-1}$) and C_i^c and C_a^c the intercellular and ambient CO_2 mole fraction (in units of μmol mol^{-1}). The validity of this equation is restricted to typical daytime conditions, when $C_a^c > C_i^c$ (i.e., during periods with net CO_2 uptake).

Eq. (2) shows that differences in LRU may be driven by the differences in two dimensionless ratios, (1) the stomatal/internal conductance to COS, and/or (2) the intercellular/ambient CO_2 concentration, which can be used to formulate hypotheses on how drought could affect the LRU.

It is well established that, with increasing drought stress, stomatal conductance is reduced to limit water loss (Gollan et al., 1985; Turner et al., 1985) and to prevent leaf water potentials from becoming too negative, potentially resulting in hydraulic failure.

In contrast to stomatal conductance, little is known about the response of internal conductance to drought. Spielmann et al. (2023) found drought to reduce g_i^s in two soybean varieties, however considerably less than g_s^s. More is known about drought effects on the mesophyll conductance, which conceptually represents one component of internal conductance (the other being related to the enzymatic consumption by carbonic anhydrase (CA) activity (Wehr et al., 2017). Overall, available data suggest that mesophyll conductance decreases under drought stress, often as fast as stomatal conductance (Flexas et al., 2008; Jones, 1973; Keenan et al., 2010). Thus, we hypothesize that drought will lead to clear reductions in both $g_s^s$and g_i^s. However, we currently lack sufficient prior information to hypothesize on whether these reductions will be proportional. Sun et al. (2024) observed proportional reductions during a heatwave, which left the $\frac{g_s^s}{g_i^s}$ ratio unchanged. Alternatively, g_s^s may decline more strongly than g_i^s, as reported by Spielmann et al. (2023), which would cause the $\frac{g_s^s}{g_i^s}$ ratio to decline. It is also possible that the $\frac{g_s^s}{g_i^s}$ ratio might even increase due to a stronger reduction in g_i^s.

In addition to the conductances, the second component of Eq. (2), $\frac{C_i^c}{C_a^c}$, can also influence the LRU in various ways in response to drought. The ratio $\frac{C_i^c}{C_a^c}$ can be reduced with increasing drought as stomatal conductance declines in early drought stages, while non-stomatal limitations are not expected yet (Gollan et al., 1985; Turner et al., 1985). This decline in $\frac{C_i^c}{C_a^c}$ would lead to a reduction of LRU. However, when the drought becomes more severe, carboxylation could also be down-regulated, thereby maintaining the $\frac{C_i^c}{C_a^c}$ ratio and the LRU constant. In an even more extreme drought scenario, one could imagine carboxylation being shut down, leading to an increase in the $\frac{C_i^c}{C_a^c}$ ratio (Brodribb, 1996) and thus to an increase in LRU. Therefore, we hypothesize that changes in LRU mediated by changes in the $\frac{C_i^c}{C_a^c}$ ratio depend on the severity of the drought stress, and on the plant's strategy for tolerating reductions in the leaf water potential (iso to anisohydric spectrum; Hochberg et al. (2018)). Taken together we hypothesize that the response of LRU to changes in soil water content (SWC) will depend on the direction and magnitude of the changes in $\frac{g_s^s}{g_i^s}$ and $\frac{C_i^c}{C_a^c}$. To address these hypotheses, here we investigate the LRU responses to a drought gradient for two mountain tree species, *Pinus sylvestris* L. and *Juniperus communis* L. These species are important and dominant in the European mountain forests and sensitive to climate change related weather extremes, like drought events (Brichta et al., 2024; Tumajer et al., 2021).

Our aim is to deepen our understanding of the underlying processes controlling the LRU by studying the behavior of $\frac{g_s^s}{g_i^s}$ and $\frac{C_i^c}{C_a^c}$ in response to increasing drought.

2. Methods

2.1. Plant material

For this experiment two-year old *Pinus sylvestris* L. (hereinafter referred to as pine) (mean height of 14 cm ± 4 cm) and *Juniperus communis* L. (hereinafter referred to as juniper) (mean height of 28 cm ± 6 cm) seedlings derived from the Landesforstgarten Bad Häring, Tirol, were used. The trees came with little soil containing 50 % white peat, 30 % black peat and 20 % wood fiber, which was amalgamated with a mixture of ¾ common soil ('Patzer Erden Blue Substrate' Type: Blue Container, and ¼ soil from the nearby forest-atmosphere-interaction-research (FAIR) site (Platter et al., 2024), where pine and juniper are the most abundant woody species. The plants were potted in VCE14 pots (Pöppelmann GmbH & Co. KG, Lohne, Germany), which were heated to 60 °C for 22 h to remove residual volatile compounds. All plants were kept outside in the botanical garden of the Innsbruck University (47.27°N, 11.38°E, 620 m a.s.l.) for about two months (March - April). Afterwards, the plants were transferred to a phytotron chamber at the ExpoSCREEN facility (Roy et al., 2021) at Helmholtz Munich in Neuherberg, Germany, where the experiment took place. In the phytotron chamber the plants could gradually adapt to the later experimental settings with respect to relative humidity (RH), light and irrigation (one month for pine (May), two months for juniper (June - July), but with identical gradual adaptation to the experimental circumstances in the last weeks). The junipers suffered from magnesium deficiency during the acclimatization phase and were therefore treated with a solution of magnesium, manganese and other trace elements, namely 'Hakaphos rot' (Compo Expert GmbH, Münster, Germany) in the composition of 1 g solved in 1 L of water, sprayed once during the last acclimatization week under low light conditions.

2.2. Phytotron chamber settings

The experiment was conducted using the VOC-SCREEN facility which was installed inside a second ExpoSCREEN chamber (Jud et al., 2018).

Here, the plants were placed in individual gas-tight glass cuvettes. The stainless-steel base of each cuvette contained different feed-throughs where irrigation and gas tubes as well as electrical cables could pass. All tubing to and from the cuvettes were made of either PTFE or PFA Teflon®. Temperature and RH sensors were available in each cuvette (DKRF400, Driesen + Kern GmbH, Bad Bramstedt, Germany), as were sensors to measure the SWC (5TM soil moisture and temperature sensor, Decagon Devices Inc., Pullman, WA, USA, typical soil moisture value accuracy of $\pm 0.03\ m^3\ m^{-3}$). Further information on the facility and setup can be found in Jud et al. (2018).

The drought experiment was carried out twice, first with the pines (07.06.2024 till 09.07.2024) and afterwards with the junipers (10.07.2024 till 05.08.2024). While the pines were measured, the junipers were kept in an acclimatization chamber, where the climate was kept similar to the period when both plants were still outside and was only increased towards the drought conditions in the last weeks as done for the pines. During the experiment the plants were arranged in four tables, with six cuvettes on each table. Five of these cuvettes contained plants, while one contained a soil-only pot (20 plants assumed to be biological replicates and four soil-only pots). Each table was assigned a drought treatment, ranging from severely drought stressed to a control treatment. The target SWC for each cuvette (six per table) was set to 5 % - 10 % for table one, 10 % - 15 % for table two, 20 % for table three and 35 % for table four (Figure S1). The plants of each table were watered via drip tubes directly in the soil with a different amount of water, depending on the target SWC of the tables, every third day after peak light intensity (around 16:00 UTC, 700 μmol $m^{-2}\ s^{-1}$). Air temperature and relative humidity (RH) within the phytotron chamber were chosen to mimic an average summertime diurnal cycle at the FAIR site, based on measurements taken from June till August 2023 (Platter et al. 2024). Air temperature ranged between 17 °C (± 1.5 °C) and 27 °C (± 1.5 °C), RH between 38 (± 9) % and 75 (± 2) %. The photosynthetic photon flux density (PPFD) was set between 0 and 700 μmol $m^{-2}\ s^{-1}$ (± 5 %) (Figure S2). The maximum PPFD value was limited by the lighting system of the phytotron chamber and is considered to be representative for typical within canopy conditions in a natural forest ecosystem. The air flow through the cuvettes was controlled with mass flow controllers (Mass Stream D-6361, *M + W* Instruments GmbH, Leonhardsbuch, Germany) at a rate of 6 L min^{-1} for the drought cuvettes and for the control cuvettes in the juniper experiment, and 7 L min^{-1} for the control cuvettes in the pine experiment. The elevated flow in the control treatment was to avoid condensation during the day, when unstressed plants transpire most. Furthermore, a slight over-pressure was maintained in the cuvettes throughout the experiment to preventing air leakage into the cuvettes (Jud et al., 2018).

2.3. Dry mole fraction measurements

COS dry mole fractions were measured at the outlet of each flow-through cuvette using a dual quantum cascade continuous-wave laser absorption spectrometer (QC-TILDAS-DUAL, Aerodyne, Billerica (MA), USA). The laser was operated at a wavenumber of ~2056 cm^{-1}, a pressure of ~2.67 kPa (regulated using a built-in pressure controller) and a controlled temperature of the optical bench and housing of 25 °C. This resulted in a signal-to-noise ratio of 15–16 at an integration time of 1 s. To minimize laser drift, the instrument was housed in a temperature-regulated custom-built case (DE Casebuilder.com GmbH, Hamburg, Germany). Absorption spectra were fitted at a frequency of 1 Hz. The storage of the calculated gas dry mole fractions, switching of zero/calibration valves and other system controls, were realized by the TDLWintel software (Aerodyne, USA). The instrument was zeroed every 30 min for 1 min using COS-free technical air. The absence of COS in the zero-air cylinder was verified using a certified span gas with a known COS mole fraction obtained from the National Oceanic and Atmospheric Administration.

Additionally, CO_2 and H_2O concentrations were measured both at the inlet and outlet of the cuvettes with an infra-red gas analyzer (LI-840A, LI-COR Biosciences, Lincoln (NE), USA).

Through a valve switching system, each cuvette containing a plant was sequentially sampled for 5 min, while the cuvettes with only soil were measured for 10 min. Measurements started with the five plant cuvettes, followed by the soil-only cuvette for each drought level corresponding to a treatment table (first table: plant, plant, plant, plant, plant, soil; next table: plant, plant, etc.). Every table was thus sampled for a total of 35 min and the maximum temporal separation between measurements from soil and plant cuvettes was 25 min.

2.4. Leaf area and biomass determination

All needles were harvested immediately after the experiment. Some of these were used to determine the plant's leaf-area (LA). These needles were scanned on a flatbed scanner (4800 × 4800 dpi, LiDE 220, Canon, Tokio, Japan) and LA was calculated with a proprietary imaging software (2018, Image Analyst). All needles were then dried at 60 °C and their dry weight was determined once it had reached a steady state (using a 0.01 g precision balance, EG 220-3NM, Kern & Sohn GmbH, Germany). The dry weight and LA of the subsamples were upscaled to the full dry weight of all needles of a plant. Changes in LA due to needle coloring during the experiment were taken into account by estimating the loss of green needles from pictures of the plants taken at different angles before and after the experiment. Lastly, although efforts were made to select plants that were as similar as possible, minor differences among individuals, especially considering the leaf area, were inevitable (Figure S3).

2.5. $\delta^{13}C$ determination

At the start and end of the experiment, the newest established needles were sampled randomly and grained to determine the natural abundance of the stable isotope ^{13}C. The isotope was determined in 1.3 mg aliquots of 10 homogenized needles per plant using an isotope ratio mass spectrometer (IRMS) (delta V Advantage, Thermo Fischer, Dreieich, Germany) coupled to an elemental analyser (EURO EA, Eurovector, Milan, Italy) (Nickel et al., 2017). A lab standard (acetanilide), included in each sequence at intervals and at different weights, was used for calibration and to determine the isotopic linearity of the system. The laboratory standard itself was calibrated against several suitable international isotopic standards (IAEA; Vienna). At the end of each run, international standards covering $\delta^{13}C$ and C contents of all samples were used for a final correction of the isotope values.

2.6. Data-analysis

Of the 5 min (or 10 min) of data per cuvette measurement, only the 60 s before the last half minute were used for the gas exchange calculations in order to prevent potential signal contamination from the previous cuvette influencing the results. Of the zero-air data we used the last 30 s. Moreover, after irrigation or opening of the climate chamber, a time window of 30 min was removed from the utilized data. Due to a failure in the irrigation system of cuvette no 10, these plant measurements were excluded. In addition, cuvette no 15 during the junipers experiment was excluded, as the corresponding plant died early during the experiment.

Fluxes of COS and CO_2 were calculated using Eq. (3).

$$F = \frac{\left(\left(c_{out_{plant}} - c_{in_{plant}}\right) - \left(c_{out_{soil}} - c_{in_{soil}}\right)\right) * \rho_m * q}{LA} \quad \text{(Eq. 3)}$$

with $\left(\left(c_{out_{plant}} - c_{in_{plant}}\right) - \left(c_{out_{soil}} - c_{in_{soil}}\right)\right)$ being the dry mole fraction difference between plant and soil measured in temporal proximity with similar SWC as the specific plant. Here we assume that $c_{in_{plant}} = c_{in_{soil}}$ when using the quantum cascade laser data (i.e., cuvette outlet COS, CO_2 and

H_2O dry mole fraction). The molar density of the respective gas at the measurement temperature and pressure is represented by ρ_m (mol m^{-3}), q is the air flowrate ($m^3 s^{-1}$) into the cuvette and LA the plant leaf area (m^2).

In the absence of plants, the dry mole fraction of COS and CO_2 measured at the outlets of the soil-only cuvettes are solely the result of soil microbial activity not related to the plant system. Subtracting these concentrations from those measured at the outlets of the cuvettes containing plants (Eq. (3)) is thought to provide a flux estimate of the net above- and below-ground plant exchange for CO_2 and COS. For CO_2, this approach neglects the priming effect of root exudates on soil heterotrophic respiration in the cuvettes containing soil and plants, which leads to an underestimation of the net plant CO_2 uptake (Hochberg et al., 2018). For COS, Kitz et al. (2024) found that the soil emission was reduced in the presence of plant roots. This suggests that either the roots, which contain enzymes of the carbonic anhydrase family, directly consume COS or that root exudates stimulate soil microbial COS uptake. Therefore, subtracting the soil-only cuvette concentrations may overestimate the plant COS uptake. These biases might propagate into the LRU leading to an overestimation of magnitude depending on the flux biases magnitude (Figure S4).

Resistances (R) were calculated by assuming a negligible boundary resistance, as the cuvette inlet flowrate was high enough and the cuvettes were well ventilated. The internal resistance for COS was calculated according to:

$$R_i^s = R_t^s - R_s^s \quad \text{(Eq. 4)}$$

with R_t^s the total resistance against COS:

$$R_t^s = \frac{\chi\mathrm{COS}}{F_{cos}} \quad \text{(Eq. 5)}$$

The stomatal resistance, R_s^s, was calculated using the conversion factor from water to COS according to Stimler et al. (2010):

$$R_s^s = 1.94 * R_s^w \quad \text{(Eq. 6)}$$

$$R_s^w = \frac{1}{g_s^w} = \frac{VPD}{E * P} \quad \text{(Eq. 7)}$$

with E the transpiration in mmol m^{-2} s^{-1}, VPD the vapor pressure deficit in kPa, and P the pressure in kPa calculated as done by Vesala et al. (2022). These resistances were used to calculate the corresponding conductances (g), the respective inverses.

Intercellular CO_2 mole fractions C_i^c were calculated by applying the Ternary correction (Baartman et al., 2025; Von Caemmerer and Farquhar, 1981).

$$C_i^c = \frac{\left(g_s^c - \frac{E}{2}\right)C_a^c + A}{g_s^c + \frac{E}{2}} \quad \text{(Eq. 8)}$$

with g_s^c the stomatal conductance to CO_2, C_a^c the ambient CO_2 concentration, and A the net assimilation rate measured with the IRGA instrument and calculated with the theory of Von Caemmerer and Farquhar (1981). The stomatal conductance to CO_2 can be calculated from that of water g_s^w according to:

$$g_s^c = \frac{g_s^w}{1.6} \quad \text{(Eq. 9)}$$

The LRU was determined during the periods of maximum light (9:00 – 16:00 UTC) using the re-arranged Eq. (1). To this end, GPP and the COS flux were derived using a temperature-dependent nighttime flux partitioning approach inspired by Reichstein et al. (2005). The fluxes between 20:00 – 05:00 UTC (when the light in the phytotron chamber was turned off) were fitted to a temperature response function using MATLAB's *fitlm* function. These temperature-dependent linear functions were used to determine the daytime (in our experiment 9:00 – 16:00 UTC) respiration and COS soil emission. As the experiment focused primarily on plant fluxes while minimizing soil contributions, the fluxes from soil-only chambers were subtracted from those of the combined plant–soil cuvettes as described above. Nevertheless, small net nighttime COS uptake were still observed after subtraction, consistent with the findings of Kitz et al. (2024).

To correct for this underestimation of the uptake COS flux, we subtracted the estimated COS soil emissions from the daytime flux. Subtracting respiration and estimated COS soil emission from the daytime CO_2 and COS fluxes, enabled us to derive the daytime GPP and the COS uptake flux of the plants. Along with COS and CO_2 mole fractions measured at the plant cuvette outlet, these were used to calculate the LRU (Eq. (1)).

For the analysis, only LRU values with negative COS and CO_2 daytime fluxes were included. Moreover, only data within the 95 % percentile range were retained and data where $\frac{C_i^c}{C_a^c}$ was above 1 was also neglected. The LRU determined this way was compared to the LRU calculated using Eq. (2) as done in Wohlfahrt et al. (2022). For the pines, additionally a linear perturbation theory was used on Eq. (2) to address the contribution of the COS conductance and CO_2 concentration ratios to the LRU drought response (Equation S1).

Eventually, for the analysis, plants were not analyzed by drought treatment, grouped by table, since maintaining identical soil water contents amongst the replicates of each table proved difficult given differences in LA (up to a factor of 2, Figure S3) and thus transpiration and water loss. Instead, plants were grouped independently of their assigned table by their SWC resulting in a full drought gradient (Kreyling et al., 2018), ranging from 1 % to 40 % SWC (Figure S5). Data with SWC values outside this range were excluded. This excluded 2.64 % of the total dataset. For clear visualization and linear regression analysis the data was grouped into 15 equally n-sized bins of SWC and thus not by temporal changes over the experimental period. Consequently, plants shifted between drought bins over time due to variation in transpiration and irrigation (e.g., a plant had a SWC of 25 % in the first week, but later dried out to a SWC of 20 %) (Figure S5).

Changepoint detection was performed to identify shifts in linear dependences using the method described in Barr et al. (2013). Uncertainty and robustness of this method were tested by bootstrapping (nboots = 1000) resulting in a relative uncertainty of 4.71 % and a coefficient of variation of 2.51 %.

Data processing was done in MATLAB© R2023a. Linear regressions and p-values of slopes were calculated using MATLAB's *fitlm* function. To determine statistical significances between means, the Anova test (lm_joint) was used, while for testing for significant differences between medians, the Mann–Whitney U test (ranksum) was conducted. Lastly, the feature importance's of PPFD, temperature, and SWC for COS flux were determined with a random forest analysis using the MATLAB function TreeBagger with Out of bag (OOB) sampling. A total of 100 trees were used, as with this number the OOB mean squared error stabilized.

Complementary to the $\frac{C_i^c}{C_a^c}$ data gathered with the gas exchange experiment, we calculated the time integrated $\frac{C_i^c}{C_a^c}$ using the $\delta^{13}C$ data via the method described in Cernusak et al. (2008), Farquhar et al. (1982) and Farquhar and Richards (1984). An atmospheric $\delta^{13}C$ value of −8 ‰ was used (Global Monitoring Laboratory).

3. Results

3.1. LRU and fluxes

The LRU, calculated using the fluxes (Eq. (1) rewritten), did not change significantly with increasing drought for pine (Fig. 1) and had a median daytime value of 1.47, a median absolute deviation (MAD) of

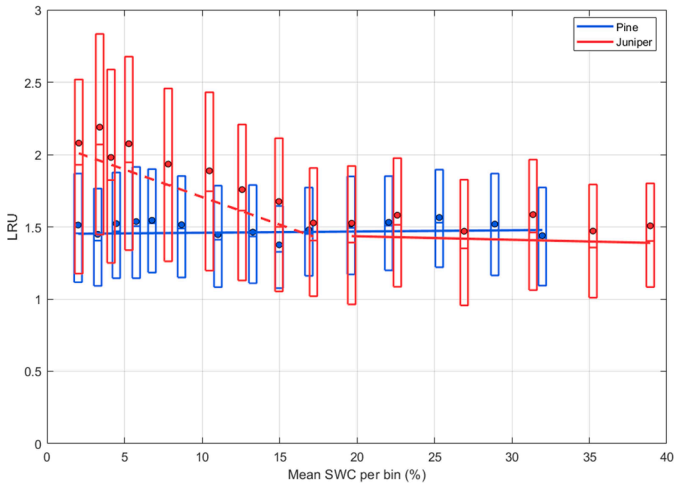

Fig. 1. Leaf relative uptake (LRU) against soil water content (SWC) for pine (blue) and juniper (red) with boxes indicating the 25 % - 75 % percentiles, dots showing the means per bin of SWC and linear fits through the medians (lines). Only daytime (9:00 – 16:00 UTC) data was used. In the case of juniper, a changepoint at 17.71 % SWC (p-value $<$ 0.0001) was found. Below this changepoint LRU decreased with increasing SWC (dashed line, slope of -0.038 ± 0.0048 and R^2 of 0.90), above 17.71 % SWC the LRU remained approximately constant as SWC increased.

0.34 and an interquartile range (IQR) of 0.69. This stable LRU across the drought gradient aligns with the linear decrease in both COS and CO_2 daytime fluxes as drought intensifies (Fig. 2). The slopes of the COS and CO_2 fluxes as a function of SWC were not significantly different and thus resulting in a stable LRU (-0.186 pmol m^{-2} s^{-1} per unit SWC for COS and -0.138 μmol m^{-2} s^{-1} per unit SWC for CO_2). During nighttime, a decrease in COS uptake flux was observed (slope: 0.042 pmol m^{-2} s^{-1} per unit SWC) across the drought gradient. Notably, non-zero COS fluxes were measured even in the lowest SWC bins, consistent with the non-zero stomatal conductance observed at similar SWC levels. Similarly, respiration showed a decreasing trend with increasing drought (Fig. 2).

For juniper the LRU remained stable at SWC values above 17.71 % with a changepoint p-value of $<$ 0.0001. The median LRU in this SWC range was 1.41 (MAD 0.43, IQR 0.88) and was significantly different (p value $<$ 0.0001) from the LRU found in pine. For SWCs lower than 17.71 %, the slope of the SWC vs. LRU relationship for juniper was -0.038 (p-value of $<$ 0.001) and the R^2 value was 0.89. As with pine, the LRU response of juniper was reflected in the COS and CO_2 fluxes with significant changepoints (p-value $<$0.0001) separating constant fluxes per SWC unit from linearly decreasing fluxes per SWC unit. These changepoints occurred at 25.58 % SWC and 21.67 % SWC for COS and CO_2 respectively, which are slightly higher than the changepoint found for the LRU. The fluxes at the lower bound of the changepoints showed smaller daytime magnitudes and slopes (slopes of -0.0673 pmol m^{-2} s^{-1} per unit SWC for COS and -0.0876 μmol m^{-2} s^{-1} per unit SWC for CO_2) compared to pine. Furthermore, the slopes of the daytime CO_2 and COS fluxes of juniper were significantly different as reflected in the LRU

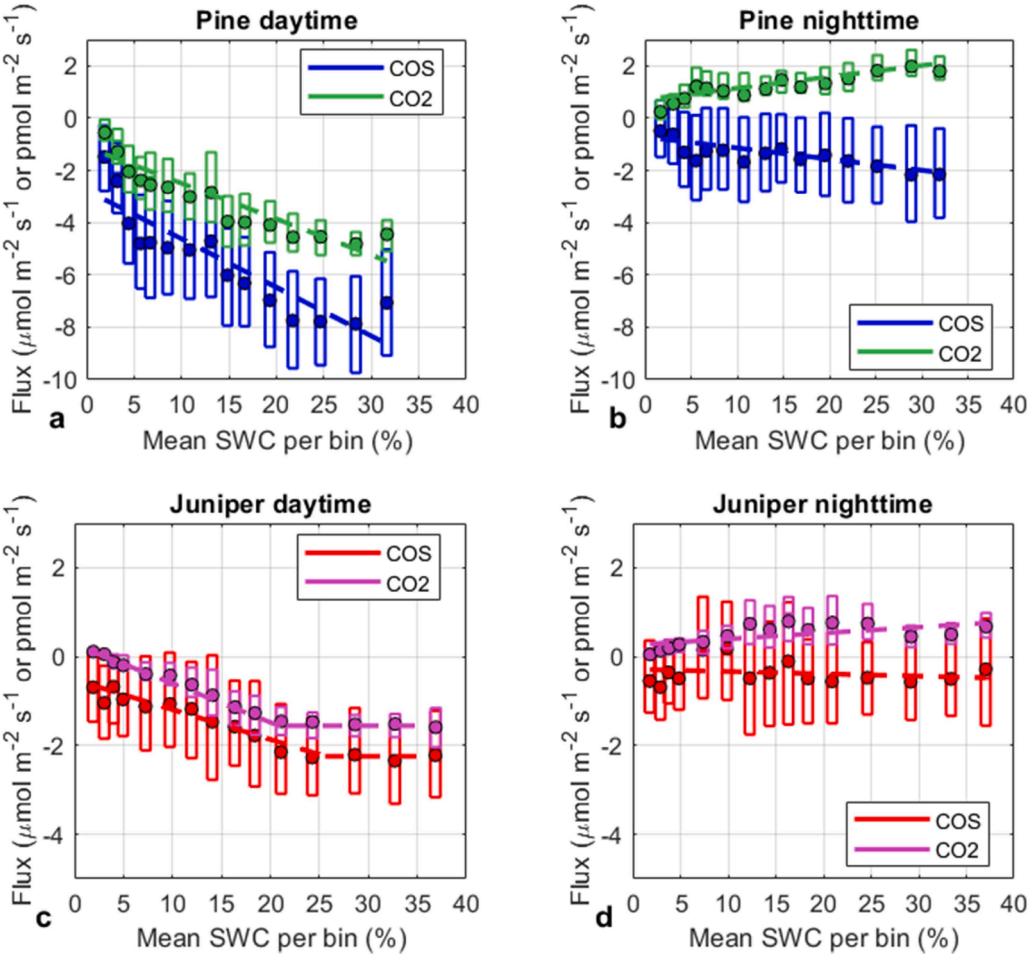

Fig. 2. Day (9:00 – 16:00 UTC) (left) and night (20:00 – 05:00 UTC) (right) COS and CO_2 fluxes (in units of *pmol* m^{-2} s^{-1} and *μmol* m^{-2} s^{-1}, respectively) for pine (upper panels) and juniper (lower panels). Boxplots show median and 25 % - 75 % percentiles, dots show mean values per bin of SWC. Negative values indicate uptake. Dashed lines show the linear fits.

(Fig. 1). The nighttime COS flux was independent of the drought gradient as the slope was not significantly different from zero (Fig. 2d). This is reflected in the nighttime g_s^s values which are close to zero across the whole drought gradient, unlike seen for the pines. In contrast, nighttime respiration decreased and tended towards zero with increasing drought as found in pine (Fig. 2b).

The drought response is further evident in the cumulative daytime COS and CO_2 fluxes (Figure S6) with pine having around 5 times higher fluxes for both compounds.

The primary driver of the diurnal cycle of COS and CO_2 fluxes was PPFD, while temperature and VPD were less important (Random Forest feature importance of 0.7 over 0.4 and 0.3 respectively for both species with RMSE of around 1.5 for pine and 0.5 for juniper). The magnitude of the uptake fluxes was dependent on the SWC. In pine, the lowest SWC bin maximum fluxes were around −4 pmol m^{-2} s^{-1} COS and −3.5 μmol m^{-2} s^{-1} CO_2 while in the highest SWC bin the daytime maxima were around −7 pmol m^{-2} s^{-1} COS and −4.5 μmol m^{-2} s^{-1} CO_2. In juniper, the uptake fluxes were significantly different than in pine with magnitudes half as large. In the lowest SWC bin, the COS flux was around −1 pmol m^{-2} s^{-1} while CO_2 fluxes were close to zero. In the highest SWC bin the daytime maxima were around −2.5 pmol m^{-2} s^{-1} COS and −2 μmol m^{-2} s^{-1} CO_2. (Figure S7). Also, the shape of the diurnal cycle changed with SWC. At lower SWC levels, the uptake peak occurred earlier in the day and was sharper. In contrast, at higher SWC levels, uptake was more evenly distributed throughout the light period (Figure S7).

3.2. Conductance and concentration ratios

To analyze the processes behind the LRU responses to drought, we also calculated the LRU using the conductance and concentration ratios as defined in Eq. (2). This equation is able to represent the LRU derived from the fluxes within a plausible LRU range of 0 - 10 for both species with an R^2 value of around 0.6 (Figure S8).

When analyzing the behavior of $\frac{g_s^s}{g_i^s}$ in response to drought, differences between the two species were observed. In pine $\frac{g_s^s}{g_i^s}$ declined (with a slope of 0.01 per SWC unit and a p-value of 0.004) with increasing drought (Fig. 3a) mostly due to the decline in g_s^s (Fig. 4). Across the entire drought gradient, including well-watered conditions, $\frac{g_s^s}{g_i^s}$ values remained below 1, indicating prevailing stomatal limitations, as g_s^s values were consistently lower than g_s^i values (Fig. 4). The other component of Eq. (2), $\frac{C_i^c}{C_a^c}$, showed a significant decrease (slope of 0.0048, p-value of 0.003) with decreasing SWC (Fig. 3b). The mutual drought response across the drought gradient of $\frac{g_s^s}{g_i^s}$ and $\frac{C_i^c}{C_a^c}$ was reflected also in the linear perturbation analysis highlighting the counteracting effect of both responses resulting in the stable LRU (Figure. S8). The decrease in $\frac{C_i^c}{C_a^c}$ with increasing drought is also reflected in the $\delta^{13}C$ data as being less negative at the end of the experiment compared to the samples taken pre-drought (Figure S10). The $\frac{C_i^c}{C_a^c}$ calculated with the corresponding $\Delta^{13}C$ (Figure S11) reflected the exact same decreasing pattern with increasing drought (Figure S12).

Also in juniper $\frac{g_s^s}{g_i^s}$ decreased (Fig. 3a) driven by a decrease in g_s^s (Fig. 4a). However, the decrease was only observed for SWC < 17 %. This decrease in $\frac{g_s^s}{g_i^s}$ (with a slope of 0.02 per SWC unit and a p value < 0.001) led to an increase of the LRU for this lower SWC range. For SWC > 17 %, the $\frac{g_s^s}{g_i^s}$ ratio was stable and around 1 which highlights a co-limitation by g_s^s and g_i^s at these higher SWC levels. Unlike what was found in pine, in juniper $\frac{C_i^c}{C_a^c}$ did not change significantly over the drought gradient (Fig. 3b). This pattern was consistent with the $\delta^{13}C$ data (Figure S10), from which calculated $\frac{C_i^c}{C_a^c}$ values likewise showed no trend with SWC (Figure S12).

Further investigations into the response of $\frac{g_s^s}{g_i^s}$ to drought revealed that during daytime g_s^s was around three times higher in pine than in juniper for plants with water availability higher than 25 % (Fig. 4a). This difference becomes smaller in plants with lower water availability, as in pine g_s^s was reduced earlier in the drought treatment than in juniper where a reduction in g_s^s was mainly seen for a SWC below about 17 %. In the early light hours, in well-watered pine trees a small rise in g_s^s was seen, while in water limited pine plants and in juniper this was not observed (Figure S13, S14). In addition, the magnitude of g_i^s differed

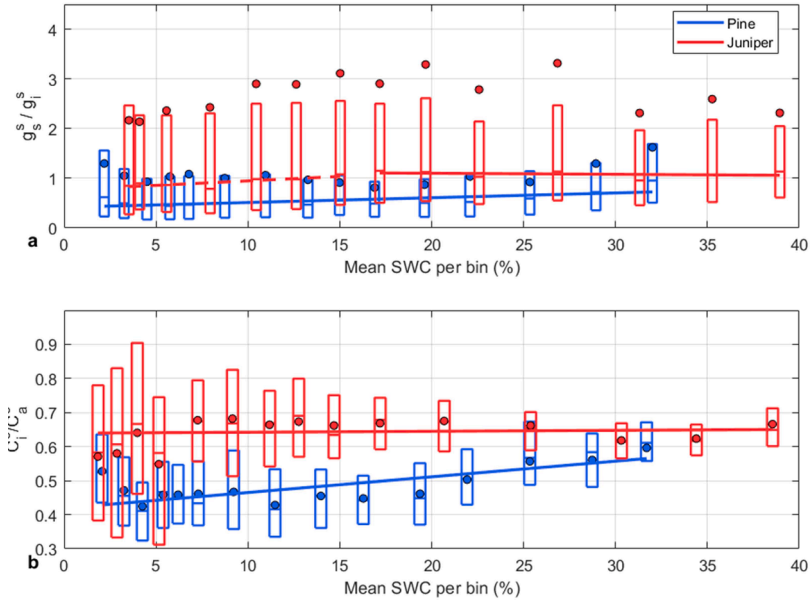

Fig. 3. a) $\frac{g_s^s}{g_i^s}$ and b) $\frac{C_i^c}{C_a^c}$ against SWC bin for pine (blue) and juniper (red). Boxplots show medians and 25 % - 75 % percentiles, dots illustrate mean values per bin of SWC. Only daytime (9:00 – 16:00 UTC) data was used. In a, in the case of juniper, a changepoint was detected at 17.17 % SWC (p-value < 0.0001). Below this point, the $\frac{g_s^s}{g_i^s}$ ratio increased with increasing SWC (dashed line, slope of 0.018 ± 0.0061 and R^2 of 0.64), after this point the $\frac{g_s^s}{g_i^s}$ ratio remained approximately constant as SWC increased (solid line).

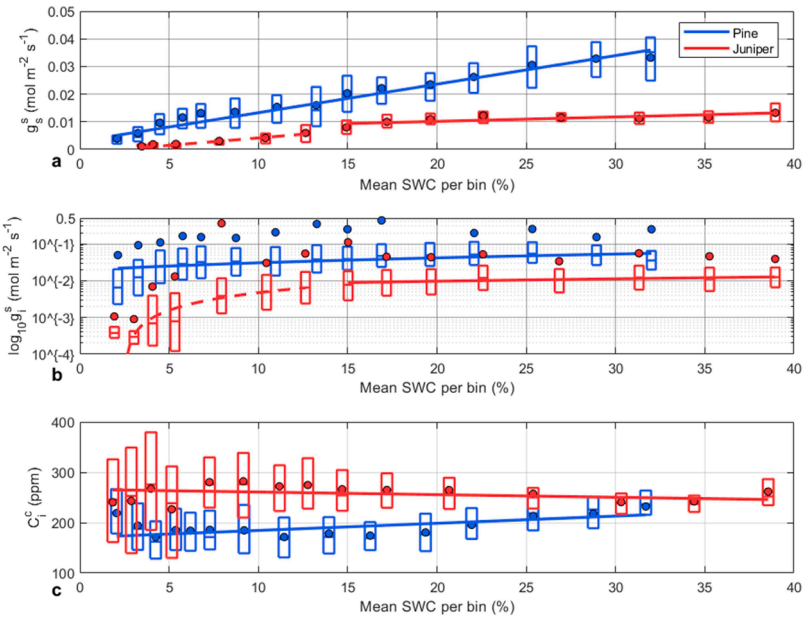

Fig. 4. Median daytime (9:00 – 16:00 UTC) stomatal (g_s^s) and internal conductance (g_i^s) (in units of mol m^{-2} s^{-1}) on a log scale, and internal concentration (C_i^c) for pine (blue) and juniper (red) with 25 % - 75 % percentile ranges. Means are depicted as dots. In juniper, significant changepoints of $g_s^s$and g_i^s were detected around a SWC of 14.9 % as indicated with the dashed lines (slope of g_s^s 0.0003 ± 0.0001 p-value of 0.002 and R^2 of 0.93) and solid lines for zero slope lines.

between the species with again higher conductance values for pine. In both species g_i^s decreased with increasing drought (Fig. 4b). During nighttime, both species' conductances were not influenced by SWC. Note that in the extreme low SWC regime (Figure S14, bins 1 and 2), conductances are close to but still non-zero which is reflected in the minute fluxes at these low SWC values (Fig. 2).

The daytime values of $\frac{C_i^c}{C_a^c}$ were similar in both species for SWC > 25 %. For plants experiencing a lower SWC, the ratio was higher in juniper than in pine with an exception for plants with SWC < 3.5 % (Figure S15). Moreover, a temporal increase during daytime hours (9:00 – 16:00 UTC) in $\frac{C_i^c}{C_a^c}$ was seen in juniper in these drier plants due to an increase in C_i^c (Fig. 4c)

4. Discussion

A good understanding of species-specific changes in LRU in response to drought is essential for GPP estimates using the COS proxy, especially since the mechanisms of stress remain poorly understood despite their importance for these estimations. To address this shortcoming, we investigated the LRU of *Pinus sylvestris* and *Juniperus communis* over a wide drought gradient. We measured COS, CO_2 and H_2O fluxes, and investigated the two main process parameters driving the LRU, i.e., the SWC dependent ratios of internal and stomatal conductance to COS, $\frac{g_s^s}{g_i^s}$, and the intercellular to ambient CO_2 concentration, $\frac{C_i^c}{C_a^c}$.

4.1. Stomatal conductance

In line with the findings of numerous drought experiments (Chaves et al., 2003; Gollan et al., 1985; Jones, 1998; Turner et al., 1985) and our own hypothesis, we observed a significant decrease in g_s^s as drought increased in both species (Fig. 4a). This reduction in g_s^s was accompanied by the observed decrease in uptake fluxes (Fig. 2). The decline in g_s^s coincided with a decline in $\frac{C_i^c}{C_a^c}$ with increasing drought (Fig. 3), suggesting no or minor non-stomatal limitation of the fluxes as apparently photosynthesis continued as hypothesized for early drought stress (Gollan et al., 1985; Turner et al., 1985). Differences between the species were evident in the magnitude of g_s^s, with pine having higher absolute conductances than juniper and a dynamic and immediate response to the drought, while juniper showed responses only for SWC < 17 %.

4.2. LRU response to drought

The main goal of this experiment was to test our hypothesis of a variable LRU response to drought stress, which may possibly be different between species.

The median LRU value for C_3 species reported by Whelan et al. (2018) of 1.68 (95 % confidence interval between 0.9 and 6.2) aligns closely with the medians we found in pine (1.47 with IQR of 0.69) and juniper (1.41 with IQR of 0.88 at SWC > 17 %). Despite these LRU values being close to earlier reported values, they differed significantly between the two tested species, despite similar experimental conditions. This underscores the fact that the LRU is highly species-dependent. Furthermore, the different LRU medians that we found also demonstrate the importance of understanding the changes of the dimensionless ratios that drive LRU, $\frac{g_s^s}{g_i^s}$ and $\frac{C_i^c}{C_a^c}$. These ratios have been shown to be species-specific (Sun et al., 2022; Wohlfahrt et al., 2022).

We hypothesized that drought would lead to a clear reduction in g_s^s and assumed that also g_i^s would be reduced, but *a-priori* without knowledge of the relative decline and thus the impact on the $\frac{g_s^s}{g_i^s}$ ratio. For $\frac{C_i^c}{C_a^c}$ we hypothesized a decline during the early-stage drought stress due to the reduction in g_s^s and a constant $\frac{C_i^c}{C_a^c}$ when drought stress would become severe enough to trigger down regulation of carboxylation.

In pine, the constant LRU observed under drought stress was the result of a strong decrease in $\frac{C_i^c}{C_a^c}$, which was largely counteracted by a concomitant decrease in $\frac{g_s^s}{g_i^s}$ (Fig. 3). The initial decrease in $\frac{C_i^c}{C_a^c}$ was driven by a reduction of the intercellular CO_2 concentration C_i^c, likely due to the decrease in g_s^s and continuous photosynthetic demand. However, a change point was detected at approximately 12 % SWC, where C_i^c began to increase with further drought (Fig. 4c). However, as simultaneously C_a^c increased due to the decrease in net CO_2 uptake within the cuvette, this did not change the overall declining trend of $\frac{C_i^c}{C_a^c}$ with decreasing

SWC. This phenomenon, also reported by Brodribb (1996), was likely a consequence of the progressive shutdown of carboxylation processes. The overall decrease in $\frac{C_i^c}{C_a^c}$ suggests that, despite the clear increase in diffusional limitations (as evidenced by the decrease in g_s^s), photosynthesis declined less than expected. This is also supported in the less negative $\delta^{13}C$ values found at the end of the drought treatment (Figures S10, S12). This suggests that non-stomatal limitations played a minor, if any, role in pine under drought conditions. The reduction of $\frac{C_i^c}{C_a^c}$ with increasing drought would force the LRU to decrease. However, as mentioned above, in the pine experiment not only $\frac{C_i^c}{C_a^c}$ but also the $\frac{g_s^s}{g_i^s}$ ratio decreased with declining SWC (Fig. 3). This decrease in $\frac{g_s^s}{g_i^s}$ with increasing drought, as was also found to occur in the drought experiment by Spielmann et al. (2023), was primarily driven by g_s^s. The stomatal conductance decreased linearly with increasing drought to minimize water loss, while g_i^s exhibited a delayed response, decreasing at SWC levels below 7.5 % (Fig. 4a, b). Additionally, as the ratio of $\frac{g_s^s}{g_i^s}$ was lower than 1 during the whole pine experiment, this indicates that COS uptake was primarily limited by g_s^s and not by g_i^s. A decrease in $\frac{g_s^s}{g_i^s}$, would force the LRU to increase with increasing drought.

Remarkably, the simultaneous and linear adaptation of both $\frac{g_s^s}{g_i^s}$ and $\frac{C_i^c}{C_a^c}$ across the drought gradient resulted in an invariant LRU in pine as visualized in Figure S9 using the linear perturbation theory.

The drought response in pine contrasts sharply with the patterns observed in juniper.

Although the LRU in juniper for SWC larger than ~ 17 % also showed a relatively constant pattern, this was due to the stability of both $\frac{C_i^c}{C_a^c}$ and $\frac{g_s^s}{g_i^s}$ in this SWC range instead of their mutual adaptation (Fig. 1, Fig. 3). In contrast to pine, at these SWC levels, $\frac{g_s^s}{g_i^s}$ was approximately 1 (Fig. 3), indicating a co-limitation of similar strength of COS uptake by g_s^s and g_i^s (Fig. 4). On a side note, the $\frac{g_s^s}{g_i^s}$ for juniper is skewed in positive direction (skewness = 0.5) resulting in higher mean values than the median and percentile ranges (Fig. 3). This also affects the calculated LRU shown in Figure S8. However, with decreasing SWC, $\frac{C_i^c}{C_a^c}$ still did not change substantially, as could also be demonstrated with the $\frac{C_i^c}{C_a^c}$ calculated from $\delta^{13}C$ (Figure S12), decreasing only at very low (around 2.5 %) SWC, while $\frac{g_s^s}{g_i^s}$ declined. This decline in $\frac{g_s^s}{g_i^s}$ reflected the stomata-limited COS uptake, which led to an increase in LRU and was reflected in the COS and CO_2 fluxes, although with differing changepoints for the individual fluxes (Fig. 2). The discrepancy among changepoints was because the LRU changepoint is determined by the point at which the ratio of the two fluxes, combined with the ratio of COS and CO_2 concentrations, undergoes the most significant variation. This changepoint occurred at a lower SWC than the changepoints observed for the individual fluxes. The $\frac{g_s^s}{g_i^s}$ ratio in juniper exhibited a similar changepoint to that observed in the LRU. Unlike pine, however, C_i^c, $\frac{C_i^c}{C_a^c}$ and the $\delta^{13}C$ data in juniper showed no significant response to drought stress which is exactly the reason why the LRU increased.

The minor difference between the LRU calculated with Eq. (1) and Eq. (2) (Figure S8) can likely be attributed to an offset of the two CO_2 measuring devices (Figure S16). Since in Eq. (2) both inlet and outlet CO_2 concentrations are needed, we used the data from the IRGA, while for the calculation of the LRU from Eq. (1), we used data only from the QC-TILDAS-DUAL instrument.

4.3. Fluxes

Nighttime CO_2 emissions decreased towards zero with drought severity in both species. This was expected as with increasing drought intensity, less carbon was assimilated during daytime (Fig. 2) and thus less carbon was available for nighttime respiration (Rehschuh et al., 2022). For COS, no significant changes in nighttime fluxes were measured. This is consistent with finite nocturnal stomatal conductance, which was more or less constant under all conditions (Figure. S9). This suggests that nighttime stomatal aperture in these two species is tightly controlled to lose as little water as possible by sacrificing nighttime cooling and prioritize daytime CO_2 uptake, regardless of the SWC (Cowan et al., 1977; Lloyd and Farquhar, 1994; Wang et al., 2021). The diurnal pattern of the COS and CO_2 fluxes in both species (Figure S7) reflects the plants' stomatal behavior under drought stress. At low SWC, plants opened their stomata as soon as the illumination was switched on but closed them again soon (within approximately 5 h) to prevent water potentials from dropping to dangerously low levels. In contrast, well-watered plants maintained stomata open throughout the day, as they did not face the same risk of hydraulic failure (Lambers et al., 2019).

4.4. Experimental limitations

There were a few experimental limitations that may have contributed to uncertainties in our results:

Since only cuvette outlet concentrations of COS were measured, changes in outside COS concentrations could have affected our results. Although rapid and short-term fluctuations in external COS concentrations were unavoidable, slow sub-daily variations were minimized by calculating fluxes as the difference between the plant cuvette and its corresponding soil cuvette, matched to the same drought level and measured within a maximum of 25 min offset. However, this method of subtracting soil-only fluxes from the plant + soil fluxes, overestimated the plant's COS uptake, as COS emissions have been found to be higher in bare soil than in soil containing root matter (Kitz et al., 2024). It should be noted, however, that the species and experimental setup used in Kitz et al. (2024) differed substantially from those in the present study. Consequently, using bare soil instead of root-containing soil for both COS and CO_2 flux measurements could introduce a bias, which may either partially cancel out in the LRU, as reflecting the relative uptake of the two gases, or propagate in both directions (Figure S4). Addressing this uncertainty will require further targeted research across a broad range of plant species.

Moreover, the temperature inside the individual cuvettes was not regulated and therefore, it adjusted with respect to the regulated phytotron chamber temperature and plant evapotranspiration rates. The resulting temperature differences between the different cuvettes (< 3 °C) were considered in the data-analysis.

Lastly, seedlings were used for this experiment as the plants needed to fit into the cuvettes of the VOC-SCREEN facility. Therefore, quantitatively different outcomes may be expected for older trees. Adult trees are more resilient to drought, as in general they have a more extensive root system that is able to access a larger volume of water. Moreover, older trees have larger water and carbohydrate reserves and a smaller leaf area to sapwood ratio than small trees (McDowell et al., 2002). Therefore, the drought stress reactions could be delayed to lower SWC values in larger trees, but the qualitative findings of this study are unlikely to change in older plants as the different coping mechanisms against drought are species-specific (McDowell et al., 2013).

Nevertheless, our results emphasize the different processes responding to drought in pine and juniper enforcing the hypothesis that LRU is species-specific and can be different depending on external factors such as drought.

4.5. Outlook

While this study examined LRU variability in two species exposed to a single stressor, expanding this research to a wider range of species and environmental conditions could help generalize and parameterize these

patterns for application in carbon cycle models. Ultimately, a deeper understanding of LRU variability across species and conditions will improve our ability to predict how plants respond to environmental change and refine the role of COS in research on the global carbon cycle.

CRediT authorship contribution statement

Anna de Vries: Writing – review & editing, Writing – original draft, Visualization, Validation, Project administration, Methodology, Investigation, Formal analysis, Data curation, Conceptualization. **Felix M. Spielmann:** Writing – review & editing, Visualization, Validation, Methodology, Investigation, Formal analysis, Data curation, Conceptualization. **Albin Hammerle:** Writing – review & editing, Visualization, Methodology, Formal analysis, Conceptualization. **Judith Schmack:** Writing – review & editing, Visualization, Validation, Methodology, Investigation, Formal analysis, Data curation, Conceptualization. **Werner Jud:** Writing – review & editing, Validation, Methodology, Investigation, Data curation, Conceptualization. **Thomas Karl:** Writing – review & editing, Methodology, Conceptualization. **Jörg-Peter Schnitzler:** Writing – review & editing, Methodology, Investigation, Conceptualization. **Jana Barbro Winkler:** Writing – review & editing, Methodology, Investigation, Conceptualization. **Georg Wohlfahrt:** Writing – review & editing, Visualization, Methodology, Formal analysis, Conceptualization.

Declaration of competing interest

The authors declare that they have no known competing financial interests or personal relationships that could have appeared to influence the work reported in this paper.

Acknowledgements

We would like to thank the technical staff (in particular Baris Weber and Franz Buegger) and the gardeners (in particular Ulrich Junghans) at the Helmholtz Zentrum München, Research Unit Environmental Simulation (EUS), for assistance in the preparation and the realization of the VOC-SCREEN experiment. Moreover, we acknowledge the help of Andreas Osl from Landesforgarten Bad Häring for selecting the plants for the experiment.

AdV and JS would like to express their gratitude for the funding provided by Austrian National Science Fund (FWF, doc.funds — FWF, DOC 171 and 10.55776/P35737) as this research was funded in whole by the Austrian Science Fund (FWF), project "The Future of Mountain Forests", grant-doi 10.55776/DOC171. For the purpose of Open Access, the authors have applied a CC BY public copyright license to any Author Accepted Manuscript (AAM) version arising from this submission.

Lastly, the project was also supported by the Research Area "Mountain Regions" of the University of Innsbruck.

Supplementary materials

Supplementary material associated with this article can be found, in the online version, at doi:10.1016/j.stress.2026.101355.

Data availability

Data is available on the repository as written in the manuscript.

References

Asaf, D., Rotenberg, E., Tatarinov, F., Dicken, U., Montzka, S.A., Yakir, D., 2013. Ecosystem photosynthesis inferred from measurements of carbonyl sulphide flux. Nat. Geosci. 6 (3), 186–190.

Baartman, S.L., Driever, S.M., Wassenaar, M., Kooijmans, L.M., Ubierna Lopez, N., Mossink, L., Popa, M.E., Cho, A., Wingate, L., Röckmann, T., 2025. Isotope discrimination of carbonyl sulfide (34 S) and carbon dioxide (13 C, 18 O) during plant uptake in flow-through chamber experiments. EGUsphere 2025, 1–24.

Barr, A., Richardson, A., Hollinger, D., Papale, D., Arain, M., Black, T., Bohrer, G., Dragoni, D., Fischer, M., Gu, L., 2013. Use of change-point detection for friction–velocity threshold evaluation in eddy-covariance studies. Agric. Meteorol. 171, 31–45.

Berkelhammer, M., Asaf, D., Still, C., Montzka, S., Noone, D., Gupta, M., Provencal, R., Chen, H., Yakir, D., 2014. Constraining surface carbon fluxes using in situ measurements of carbonyl sulfide and carbon dioxide. Glob Biogeochem Cycles 28 (2), 161–179.

Berry, J., Wolf, A., Campbell, J.E., Baker, I., Blake, N., Blake, D., Denning, A.S., Kawa, S. R., Montzka, S.A., Seibt, U., 2013. A coupled model of the global cycles of carbonyl sulfide and CO2: a possible new window on the carbon cycle. J. Geophys. Res. Biogeosci. 118 (2), 842–852.

Brichta, J., Šimůnek, V., Bílek, L., Vacek, Z., Gallo, J., Drozdowski, S., Bravo-Fernández, J., Mason, B., Gomez, S., Hájek, V., 2024. Effects of climate change on scots pine (Pinus sylvestris L.) growth across Europe: decrease of tree-ring fluctuation and amplification of climate stress. Forests. 15 (1), 91. *Go to original source*.

Brodribb, T., 1996. Dynamics of changing intercellular CO2 concentration (ci) during drought and determination of minimum functional ci. Plant Physiol. 111 (1), 179–185.

Campbell, J.E., Carmichael, G.R., Chai, T., Mena-Carrasco, M., Tang, Y., Blake, D., Blake, N., Vay, S.A., Collatz, G.J., Baker, I., 2008. Photosynthetic control of atmospheric carbonyl sulfide during the growing season. Science 322 (5904), 1085–1088.

Cernusak, L.A., Winter, K., Aranda, J., Turner, B.L., 2008. Conifers, angiosperm trees, and lianas: growth, whole-plant water and nitrogen use efficiency, and stable isotope composition (δ 13C and δ 18O) of seedlings grown in a tropical environment. Plant Physiol. 148 (1), 642–659.

Chaves, M.M., Maroco, J.P., Pereira, J.S., 2003. Understanding plant responses to drought—from genes to the whole plant. Funct. Plant Biol. 30 (3), 239–264.

Cowan, I., Farquhar, G., Jennings, D., 1977. Integration of activity in the higher plant. Stomatal Function in Relation to Leaf Metabolism and Environment. Cambridge Univ Press, Cambridge, pp. 471–505.

Dai, A., 2013. Increasing drought under global warming in observations and models. Nat. Clim. Chang. 3 (1), 52–58.

Farquhar, G., Richards, R., 1984. Isotopic composition of plant carbon correlates with water-use efficiency of wheat genotypes. Funct. Plant Biol. 11 (6), 539–552.

Farquhar, G.D., O'Leary, M.H., Berry, J.A., 1982. On the relationship between carbon isotope discrimination and the intercellular carbon dioxide concentration in leaves. Aust. J. Plant Physiol. 9 (2), 121–137.

Flexas, J., Ribas-Carbo, M., Diaz-Espejo, A., Galmés, J., Medrano, H., 2008. Mesophyll conductance to CO2: current knowledge and future prospects. Plant Cell Environ. 31 (5), 602–621.

Friedlingstein, P., Le Quéré, C., O'sullivan, M., Hauck, J., Landschützer, P., Luijkx, I.T., Li, H., van der Woude, A., Schwingshackl, C., Pongratz, J., 2025. Emerging climate impact on carbon sinks in a consolidated carbon budget. Nature 1–3.

Friedlingstein, P., O'sullivan, M., Jones, M.W., Andrew, R.M., Hauck, J., Landschützer, P., Le Quéré, C., Li, H., Luijkx, I.T., Olsen, A., 2024. Global carbon budget 2024. Earth Syst. Sci. Data Discuss 2024, 1–133.

Global Monitoring Laboratory. *The data: what 13C tells us*. https://gml.noaa.gov/outreach/isotopes/c13tellsus.html#:~:text=Before%20the%20industrial%20revolution%2C%20%CE%B4%2013%20C%20of,negative%20%CE%B4%2013%20C%20value%20of%20around%20-25%E2%80%B0%29.

Gollan, T., Turner, N.C., Schulze, E.-D., 1985. The responses of stomata and leaf gas exchange to vapour pressure deficits and soil water content: III. In the sclerophyllous woody species Nerium oleander. Oecologia 65, 356–362.

Hochberg, U., Rockwell, F.E., Holbrook, N.M., Cochard, H., 2018. Iso/anisohydry: a plant–environment interaction rather than a simple hydraulic trait. Trends. Plant Sci. 23 (2), 112–120.

IPCC, 2023. Summary for policymakers. In: Lee, H., Romero, J. (Eds.), Climate Change 2023: Synthesis Report. Contribution of Working Groups I, II and III to the Sixth Assessment Report of the Intergovernmental Panel On Climate Change [Core Writing Team. IPCC (eds.)].

Jones, H.G., 1973. Moderate-term water stresses and associated changes in some photosynthetic parameters in cotton. New. Phytol. 72 (5), 1095–1105.

Jones, H.G., 1998. Stomatal control of photosynthesis and transpiration. J. Exp. Bot. 387–398.

Jud, W., Winkler, J.B., Niederbacher, B., Niederbacher, S., Schnitzler, J.-P., 2018. Volatilomics: a non-invasive technique for screening plant phenotypic traits. Plant Methods 14, 1–18.

Ke, P., Ciais, P., Yao, Y., Sitch, S., Li, W., Xu, Y., Du, X., Gui, X., Bastos, A., & Zaehle, S. (2025). Low latency global carbon budget reveals a continuous decline of the land carbon sink during the 2023/24 El Nino event. *ArXiv preprint arXiv:2504.09189*.

Keenan, T., Sabate, S., Gracia, C., 2010. The importance of mesophyll conductance in regulating forest ecosystem productivity during drought periods. Glob. Chang. Biol. 16 (3), 1019–1034.

Kitz, F., Wachter, H., Spielmann, F., Hammerle, A., Wohlfahrt, G., 2024. Root and rhizosphere contribution to the net soil COS exchange. Plant Soil. 498 (1), 325–339.

Kooijmans, L.M., Sun, W., Aalto, J., Erkkilä, K.-M., Maseyk, K., Seibt, U., Vesala, T., Mammarella, I., Chen, H., 2019. Influences of light and humidity on carbonyl sulfide-based estimates of photosynthesis. Proc. Natl. Acad. Sci. 116 (7), 2470–2475.

Kreyling, J., Schweiger, A.H., Bahn, M., Ineson, P., Migliavacca, M., Morel-Journel, T., Christiansen, J.R., Schtickzelle, N., Larsen, K.S., 2018. To replicate, or not to

replicate–that is the question: how to tackle nonlinear responses in ecological experiments. Ecol. Lett. 21 (11), 1629–1638.
Lambers, H., Oliveira, R.S., Lambers, H., Oliveira, R.S., 2019. Photosynthesis, respiration, and long-distance transport: photosynthesis. Plant Physiological Ecology, pp. 178–212.
Lloyd, J., Farquhar, G.D., 1994. 13C discrimination during CO2 assimilation by the terrestrial biosphere. Oecologia 99 (3), 201–215.
McDowell, N., Barnard, H., Bond, B., Hinckley, T., Hubbard, R., Ishii, H., Köstner, B., Magnani, F., Marshall, J., Meinzer, F., 2002. The relationship between tree height and leaf area: sapwood area ratio. Oecologia 132 (1), 12–20.
McDowell, N.G., Ryan, M.G., Zeppel, M.J., Tissue, D.T., 2013. Improving our knowledge of drought-induced forest mortality through experiments, observations, and modeling. New. Phytol. 200 (2), 289–293.
Nickel, U., Winkler, J., Mühlhans, S., Buegger, F., Munch, J., Pritsch, K., 2017. Nitrogen fertilisation reduces sink strength of poplar ectomycorrhizae during recovery after drought more than phosphorus fertilisation. Plant Soil. 419 (1), 405–422.
Orr, B.J., Dosdogru, F., Santivañez, M.S., 2024. Land degradation and drought in mountains. Safeguarding Mountain Social-Ecological Systems. Elsevier, pp. 17–22.
Pepin, N., Apple, M., Knowles, J., Terzago, S., Arnone, E., Hänchen, L., Napoli, A., Potter, E., Steiner, J., Williamson, S.N., 2025. Elevation-dependent climate change in mountain environments. Nat. Rev. Earth. Environ. 1–17.
Pepin, N.C., Arnone, E., Gobiet, A., Haslinger, K., Kotlarski, S., Notarnicola, C., Palazzi, E., Seibert, P., Serafin, S., Schöner, W., 2022. Climate changes and their elevational patterns in the mountains of the world. Rev. Geophys. 60 (1) e2020RG000730.
Piao, S., Wang, X., Park, T., Chen, C., Lian, X., He, Y., Bjerke, J.W., Chen, A., Ciais, P., Tømmervik, H., 2020. Characteristics, drivers and feedbacks of global greening. Nat. Rev. Earth. Environ. 1 (1), 14–27.
Platter, A., Scholz, K., Hammerle, A., Rotach, M.W., Wohlfahrt, G., 2024. Agreement of multiple night-and daytime filtering approaches of eddy covariance-derived net ecosystem CO2 exchange over a mountain forest. Agric. Meteorol. 356, 110173.
Rehschuh, R., Rehschuh, S., Gast, A., Jakab, A.L., Lehmann, M.M., Saurer, M., Gessler, A., Ruehr, N.K., 2022. Tree allocation dynamics beyond heat and hot drought stress reveal changes in carbon storage, belowground translocation and growth. New. Phytol. 233 (2), 687–704.
Reichstein, M., Falge, E., Baldocchi, D., Papale, D., Aubinet, M., Berbigier, P., Bernhofer, C., Buchmann, N., Gilmanov, T., Granier, A., 2005. On the separation of net ecosystem exchange into assimilation and ecosystem respiration: review and improved algorithm. Glob. Chang. Biol. 11 (9), 1424–1439.
Reif, M., Rotach, M.W., Gohm, A., Wohlfahrt, G., 2024. Carbon dioxide exchange in an idealized valley. Environ. Model. Softw. 171, 105887.
Rotach, M.W., Wohlfahrt, G., Hansel, A., Reif, M., Wagner, J., Gohm, A., 2014. The world is not flat: implications for the global carbon balance. Bull. Am. Meteorol. Soc. 95 (7), 1021–1028.
Roy, J., Rineau, F., De Boeck, H.J., Nijs, I., Pütz, T., Abiven, S., Arnone III, J.A., Barton, C. V., Beenaerts, N., Brüggemann, N., 2021. Ecotrons: powerful and versatile ecosystem analysers for ecology, agronomy and environmental science. Glob. Chang. Biol. 27 (7), 1387–1407.
Sandoval-Soto, L., Stanimirov, M., Von Hobe, M., Schmitt, V., Valdes, J., Wild, A., Kesselmeier, J., 2005. Global uptake of carbonyl sulfide (COS) by terrestrial vegetation: estimates corrected by deposition velocities normalized to the uptake of carbon dioxide (CO 2). Biogeosciences 2 (2), 125–132.
Seibt, U., Berry, J., Sandoval-Soto, L., Kuhn, U., Kesselmeier, J., 2010. A kinetic model relating the leaf uptake of carbonyl sulfide (COS) to water and CO2 fluxes and 13C fractionation. EGU Gen. Assem. Conf. Abstr.
Spielmann, F., Wohlfahrt, G., Hammerle, A., Kitz, F., Migliavacca, M., Alberti, G., Ibrom, A., El-Madany, T.S., Gerdel, K., Moreno, G., 2019. Gross primary productivity of four European ecosystems constrained by joint CO2 and COS flux measurements. Geophys. Res. Lett. 46 (10), 5284–5293.
Spielmann, F.M., Hammerle, A., Kitz, F., Gerdel, K., Alberti, G., Peressotti, A., Delle Vedove, G., Wohlfahrt, G., 2023. On the variability of the leaf relative uptake rate of carbonyl sulfide compared to carbon dioxide: insights from a paired field study with two soybean varieties. Agric. Meteorol. 338, 109504.
Stimler, K., Montzka, S.A., Berry, J.A., Rudich, Y., Yakir, D., 2010. Relationships between carbonyl sulfide (COS) and CO2 during leaf gas exchange. New. Phytol. 186 (4), 869–878.
Sun, W., Berry, J.A., Yakir, D., Seibt, U., 2022. Leaf relative uptake of carbonyl sulfide to CO2 seen through the lens of stomatal conductance–photosynthesis coupling. New. Phytol. 235 (5), 1729–1742.
Sun, W., Maseyk, K., Lett, C., Seibt, U., 2024. Restricted internal diffusion weakens transpiration–photosynthesis coupling during heatwaves: evidence from leaf carbonyl sulphide exchange. Plant Cell Environ. 47 (5), 1813–1833.
Trenberth, K.E., Dai, A., Van Der Schrier, G., Jones, P.D., Barichivich, J., Briffa, K.R., Sheffield, J., 2014. Global warming and changes in drought. Nat. Clim. Chang. 4 (1), 17–22.
Tumajer, J., Buras, A., Camarero, J.J., Carrer, M., Shetti, R., Wilmking, M., Altman, J., Sangüesa-Barreda, G., Lehejček, J., 2021. Growing faster, longer or both? Modelling plastic response of Juniperus communis growth phenology to climate change. Glob. Ecol. Biogeogr. 30 (11), 2229–2244.
Turner, N.C., Schulze, E.-D., Gollan, T., 1985. The responses of stomata and leaf gas exchange to vapour pressure deficits and soil water content: II. In the mesophytic herbaceous species Helianthus annuus. Oecologia 65, 348–355.
Vesala, T., Kohonen, K.-M., Kooijmans, L.M., Praplan, A.P., Foltýnová, L., Kolari, P., Kulmala, M., Bäck, J., Nelson, D., Yakir, D., 2022. Long-term fluxes of carbonyl sulfide and their seasonality and interannual variability in a boreal forest. Atmos. Chem. Phys. 22 (4), 2569–2584.
Von Caemmerer, S.V., Farquhar, G.D., 1981. Some relationships between the biochemistry of photosynthesis and the gas exchange of leaves. Planta 153 (4), 376–387.
Wang, Y., Anderegg, W.R., Venturas, M.D., Trugman, A.T., Yu, K., Frankenberg, C., 2021. Optimization theory explains nighttime stomatal responses. New. Phytol. 230 (4), 1550–1561.
Wehr, R., Commane, R., Munger, J.W., McManus, J.B., Nelson, D.D., Zahniser, M.S., Saleska, S.R., Wofsy, S.C., 2017. Dynamics of canopy stomatal conductance, transpiration, and evaporation in a temperate deciduous forest, validated by carbonyl sulfide uptake. Biogeosciences 14 (2), 389–401.
Whelan, M.E., Lennartz, S.T., Gimeno, T.E., Wehr, R., Wohlfahrt, G., Wang, Y., Kooijmans, L.M., Hilton, T.W., Belviso, S., Peylin, P., 2018. Reviews and syntheses: carbonyl sulfide as a multi-scale tracer for carbon and water cycles. Biogeosciences 15 (12), 3625–3657.
Wohlfahrt, G., Brilli, F., Hörtnagl, L., Xu, X., Bingemer, H., Hansel, A., Loreto, F., 2012. Carbonyl sulfide (COS) as a tracer for canopy photosynthesis, transpiration and stomatal conductance: potential and limitations. Plant Cell Environ. 35 (4), 657–667.
Wohlfahrt, G., Gu, L., 2015. The many meanings of gross photosynthesis and their implication for photosynthesis research from leaf to globe. Plant Cell Env 38 (12), 2500.
Wohlfahrt, G., Hammerle, A., Spielmann, F.M., Kitz, F., Yi, C., 2022. Novel estimates of the leaf relative uptake rate of carbonyl sulfide from optimality theory. Biogeosci. Discuss 2022, 1–13.
Wohlfahrt, G., Hammerle, A., Spielmann, F.M., Kitz, F., Yi, C., 2023. Technical note: novel estimates of the leaf relative uptake rate of carbonyl sulfide from optimality theory. Biogeosciences. 20 (3), 589–596.
Yang, F., Qubaja, R., Tatarinov, F., Rotenberg, E., Yakir, D., 2018. Assessing canopy performance using carbonyl sulfide measurements. Glob. Chang. Biol. 24 (8), 3486–3498.